Multi-Objective optimal design of a cable driven parallel robot for rehabilitation tasks

Ines Ben Hamida, Med Amine Laribi, Abdelfattah Mlika, Lotfi Romdhane, Saïd Zeghloul, Giuseppe Carbone

Multi-Objective Optimal Design of a Cable Driven Parallel Robot for Rehabilitation Tasks

Ines Ben Hamida [1,2], Med Amine Laribi [1], Abdelfattah Mlika [2], Lotfi Romdhane [2,3], Saïd Zeghloul [1], Giuseppe Carbone [4]

[1] Department of GMSC, Pprime Institute, CNRS - University of Poitiers - ENSMA - UPR 3346, Poitiers, France, Corresponding author e-mail: ines.ben.hamida@univ-poitiers.fr
[2] Mechanical Laboratory of Sousse (LMS), National Engineering School of Sousse, University of Sousse, Sousse 4000, Tunisia
[3] Department of Mechanical Engineering, American University of Sharjah, P.O. Box 26666, Sharjah, UAE
[4] Department of Mechanical, Energy and Management Engineering, University of Calabria, 87036 Rende, Italy

Abstract
This paper addresses the topological and dimensional synthesis of cable-driven parallel robots. A combined methodology for type and size optimization is proposed and applied to a cable driven parallel robot, which is intended for upper-limb rehabilitation exercises. The proposed approach deals with a set of deterministic and non-deterministic parameters within a multi-objective genetic algorithm. The proposed study aims to select a suitable architecture having optimal dimensions by considering several optimality criteria such as minimizing the cable tensions and achieving the smallest footprint. An illustrative application of the proposed synthesis approach is developed for LAWEX, a cable driven parallel robot for upper limb rehabilitation. Four different topology solutions have been considered for LAWEX robot. It is also proposed to use an additional safety criterion to select a solution on the obtained Pareto front.

Keywords
Cables driven parallel robots, dimensional synthesis, topological synthesis, performance criteria, optimization approaches

Nomenclature

CDPR	Cable Driven Parallel Robot
DOF	Degrees of Freedom
WS	workspace
m	Number of cables
$\mathbf{J}$	Jacobian Matrix
$K(J)$	Local condition number of the Jacobian Matrix
μ_j	Inverse of the local condition number
μ	Global Conditioning Index
T	Transpose
τ	Cable's tension
f	Force
M	Moment
W	Wrench
Ma	End-effector mass
g	Gravitational acceleration = 9.764 m/s²
V	Robot's size
P	Center of the moving platform
$\mathbf{I}$	Design vector of the optimization problem
$F(\mathbf{I})$	Objective functions of the optimization problem
C ($\mathbf{I}$)	Constraint functions of the optimization problem
$\mathbf{U_i}$	Orientation vector of the i^{th} cable

1. Introduction

A CDPR (cable driven parallel robot) is a parallel robot where the moving platform is suspended by flexible cables instead of classic rigid kinematic chains. This characteristic gives CDPRs valuable performances in terms of large workspace, high payload, high speed and acceleration as compared with classical parallel robots. CDPRs allow design solutions having a larger workspace when compared to parallel robots with rigid links having a comparable size. Accordingly, several researchers have been investigating this research topic.
The first CDPRs have been intended for industrial applications. RoBoCrane [1] is considered as the first cable driven parallel robot implemented in 1989 in the National Institute of Standards and Technology (NIST) of America. This 6-DOF robot has been used for several applications e.g. cutting, shaping, finishing, lifting and positioning, [1]. Lately, several CDPRs have been proposed and developed in Japan, Italy, France and Germany. For example, Falcon-7, [2] is a 6-DOF Japanese Robot with ultra-high speed and small actuators. Driven by 7 cables, this fully constrained robot was used for applications that require high precision and stiffness. Cable robots are also used for construction tasks, given their large workspace and high stiffness as compared with classic parallel mechanisms. For example, Pinto *et al.* [3] proposed SPIDERobot, a 4-DOF robot, for architectures projects. Paper [3] presented an optimization of the robot's trajectory to avoid collisions using a new Vision-Guided Path Planning System. Likewise, cable robots have demonstrated their efficiency in medicals applications, such as haptic devices and rehabilitation robots. Haptic devices require an independent control system that allows the user not only to feed information but also to receive a feedback from the machine as a felt sensation. Many haptic devices have been proposed in the literature. For example, Billette and Gosselin [4] proposed a haptic interface using a 3-DOF cable driven parallel robot for a sword-fighting simulator. RIME is a telesurgical device with a cable driven 5-dof haptic master developed at university of Padua [5]. Experiments reported by Boschetti *et al* [5] evoke the advantage of the wire driven haptic master to drive naturally and simply the surgical tool. The simplicity of assembly and reconfiguration of CDPRs, as well as their high sensitivity, light weight and large workspace make them suitable for rehabilitation tasks. Sophia-3 is a 2-DOF cable driven parallel robot used for the upper limb rehabilitation [6]. This simple device in terms of kinematics and cost can, assure shoulder rehabilitation exercises instead of complex and 3-D exoskeletons.
Passive cable devices such as CATRASYS and Milli-CATRASYS have been proposed since early '90s for the determination of the pose and orientation of mechanisms' end-effector, [7]. A recent work of Varela *et al.* [8] proposed an experimental approach using CATRASYS to characterize human walking. CUBE, proposed by Cafolla *et al.* [9], consists of 5 DOF parallel robot driven through 6 cables dedicated to clinical exercises for both upper and lower limbs. NeReBot is an upper limb neurorehabilitation device proposed by Fanin *et al.*[10]. It uses 3 cables to suspend the patient upper limb. Clinical tests by Rosati *et al.* [11] show that patients treated with the additional protocol of NeReBot are recovering faster than others treated with a classical protocol.

Dimensional synthesis is one of the challenging tasks in the design process of a mechanical system. It consists of searching for the "best dimensions" of the mechanism to fulfill the required performances. Kelaiaia *et al.* [12] proposed two different approaches for dimensional synthesis: the Atlas approach and the cost function approach. The most used technique is the cost function [12]–[18], where an optimization problem is formulated in order to minimize an objective function subject to constraint functions. Design approaches of CDPRs depend on their applications and the desired specifications, such as workspace, speed, compliance. A recent work of Laribi *et al.* [19] proposed a multi-criteria optimization of LAWEX, a CDPR dedicated to upper limb rehabilitation. The problem formulation consists in the minimization of cables tensions distribution, while following a prescribed trajectory. The solution was given using a Genetic Algorithm method implemented under MATLAB software. Lamine *et al.* [20] developed a discrete algorithm for the design optimization of a Cable Driven Leg Trainer; for gait rehabilitation. The objective of this optimization is to minimize cables tensions considering the height's difference among patients. Cables tensions of all heights have been calculated to compute the optimum power of the robot's actuators. A different optimization model was proposed by Hernandez *et al.* [21] for the design of a CDPR used for patients with shoulder problems. A

prescribed workspace was defined using the upper limb possible movements. A kinematic and wrench analyses have been carried out to determine the Jacobian matrix. The considered objective function was for the optimization of cables tensions. The problem was solved using the Estimation of Distribution Algorithm. In most the cases, the cables are considered as massless, however, in some mechanisms, long cables' masses cannot be neglected. Liu *et al.* [22] proposed a tension optimization iterative algorithm to avoid sags of long cables.

This work proposed an optimization approach of a cable driven parallel robot intended for rehabilitation of human upper limb. The paper is structured as follows: Section 2 presents the difference between our CDPR design process and the commonly used robotic mechanism design processes. The following section deals with the search of the topological structures for the CDPRs. Different characteristics and performances of cable robots are analyzed in section 4. Section 5 introduces the proposed case of study on the synthesis of LAWEX, a CDPR intended for rehabilitation tasks. A concurrent design approach combining type and dimensional synthesis is proposed and carried out. The last section presents some conclusions.

2. The proposed design approach

The mechanical design process has been the object of several works in the literature such as, just for example, [23]–[25]. The procedure described in Fig. 1 represents the proposed general conceptual design as based on the fulfillment of specific requirements or needs.

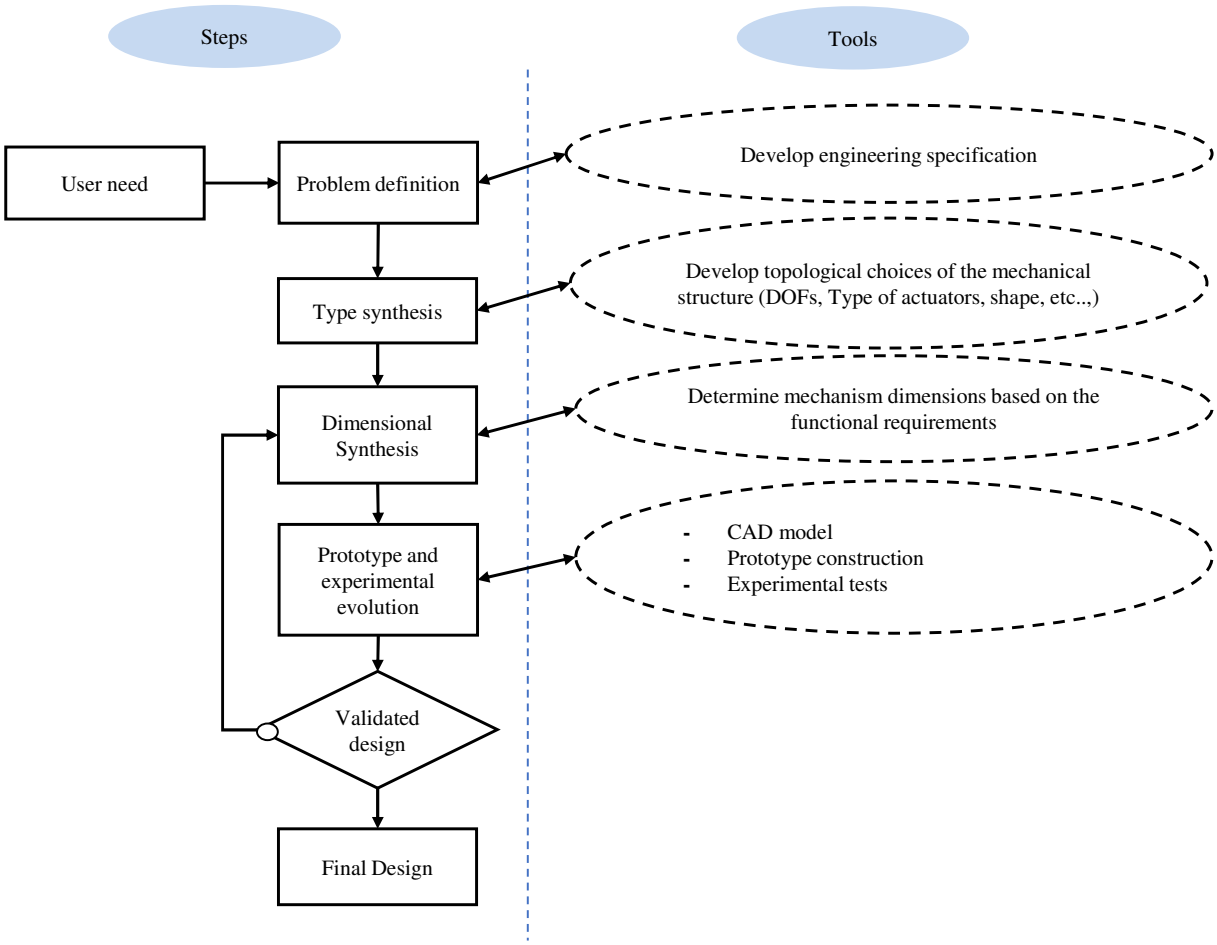

Fig. 1. Mechanical design process

First, a problem definition based on the required functional criteria by the user should be identified. A mathematical formulation of the design problem is then established for the mechanism synthesis, which is processed in two phases:

- Phase 1: Topological synthesis, which requires decisions on the main design choices concerning the number of DOFs, the actuation nature, the degree of redundancy.
- Phase 2: Dimensional synthesis related to the mechanism dimensions, where an optimization problem could be formulated to identify the best design parameters for a given required task of the mechanism.

As shown in Fig. 1, the classical design process is a sequential one, where the topological synthesis comes first followed by the dimensional synthesis. In the present work, a concurrent design approach is proposed, where the topology and dimensions of the mechanism are optimized simultaneously.

The objective of this novel design approach is to select the suitable manipulator architecture with optimized dimensions for a given task. The proposed methodology combines the type and the dimensional optimization in the same operation. The problem formulation depends on the desired application, which will define the objectives, the constraints, and the decision parameters.

3. Optimal topology search strategy

Most of the literature works on synthesis of cable driven parallel robots are interested only on dimensional optimization. However, the number of cables, the positions of the cables exit points and the positions of the cable anchor points on the moving platform, define the robot design and affects the number of DOFs as well as the device performances.

Generally, according to the number of DOFs n and the number of cables m, two main cases of CDPRs can be defined, under constrained and fully constrained CDPRs. A necessary condition but not sufficient to define an under-constrained CDPR is $m \leq n$. Typically, the end-effector of an under-constrained CDPR is still movable when actuators are locked so that external forces are necessary for static equilibrium. A CDPR is defined as fully constrained if all its n DOFs can be controlled, it requires at least $n + 1$ cables.

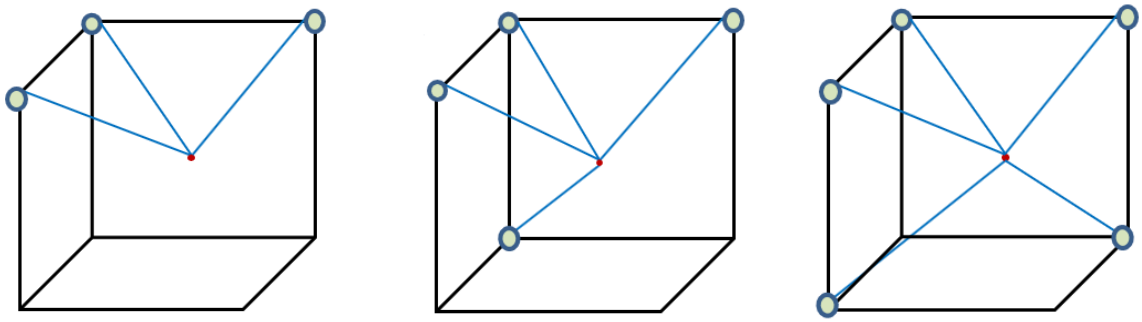

(a) (b) (c)

Fig. 2. Different configurations of CDPRs

Fig. 2 presents three possible designs of the CDPRs. The first case (a) presents an under constrained robot with 3 cables for 3 DOFs. The gravity is used in this case, to ensure positive tensions in the cables. The second case (b) is a fully constrained CDPR, which uses 4 cables to ensure the same number of DOFs as the first case. The third robot, case (c), is an over constrained CDPR, as it is using 5 cables to ensure 3 DOFs.

Redundancy of CDPRs was addressed by Merlet [26]. Despite the advantage of increasing drastically the robot's workspace, redundancy affects the kinematics and cables tensions distribution. Maintaining a positive cable tension in redundant structures, is one of the most challenging addressed issues in the literature [27].

An additional issue of cables that can affect the robot motion is the distribution of attachment points on the end-effector. Fig. 3 shows two different end-effectors with different attachment points. The first configuration uses an end-effector with two anchor points. In this case, the controllable motions of the end effector are limited to just 3 translations. In the second case, the end-effector contains one anchor

point for each cable. This feature gives the robot an additional mobility in rotation, 3 translations and one rotation are possible.

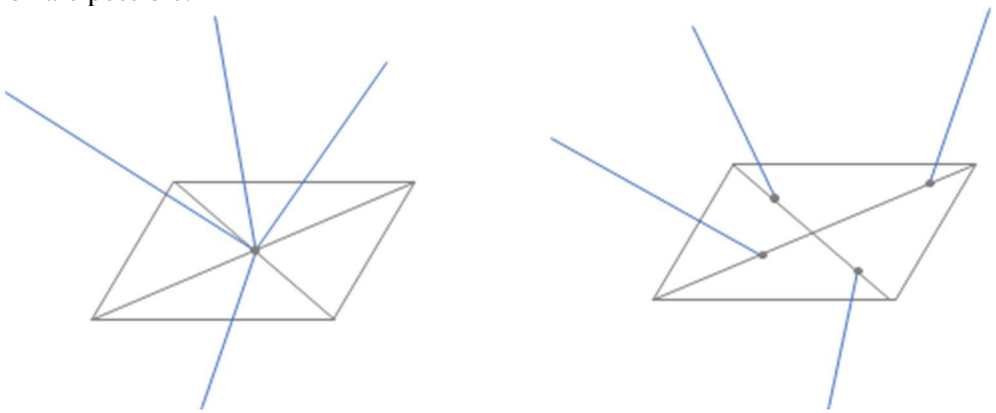

(a) (b)

Fig. 3. Different shapes of end-effector

The number of anchor points is related to the required movements of the end effector and the number of cables. A full measure of the moving object pose, i.e., position and orientation, requires 3 non-aligned points, however reducing the number of attachment points reduces the risk of cable wrapping issue. For example, for translational devices, only one attachment point is sufficient to define the pose of the end effector.

4. Optimal dimensional synthesis strategies

Dimensional synthesis deals with the determination of the mechanism dimensions according to the required performances by the designer.

A general optimization problem is formulated in order to minimize or to maximize an objective function subject to constraint functions as stated below:

$$\begin{cases} \text{Minimize/Maximize } F(\mathbf{I}) \\ \text{Subject to } C_i(\mathbf{I}) \leq 0 \\ \mathbf{I} = [x_1, .., x_n] \\ x_j^{\min} < x_j < x_j^{\max} \end{cases} \quad (1)$$

where

$F(\mathbf{I})$ is the objective function defining the criteria to optimize.

$C_i(\mathbf{I})$ are constraint functions.

$\mathbf{I} = [x_1, .., x_n]$ is the design vector defined by the set of design variables and ($x_j^{\min}$, $x_j^{\max}$) the search domain for each design variable x_j.

Depending on the application requirements, the performance criteria of an optimization problem are determined, some of them will be fixed as objectives to optimize and others as constraints. In the following, some of the mainly used performance criteria for CDPRs are introduced.

4.1. Workspace

Workspace analysis remains one of the active research items for parallel robots and especially for CDPRs. A general definition of the workspace is given by the region of space reachable by the moving platform. CDPRs have potentially a large workspace compared to the classic parallel robots. However, there is an additional constraint for CDPRs since the robot's cables can only pull on the end-effector, which requires the cables tensions to always be positive. Additional conditions can be added to the workspace, which lead to different workspaces types.

The first researches on CDPRs' workspace have been interested in wrench closure workspace (WCW) and wrench feasible workspace (WFW). WCW refers to the main characteristics of CDPRs, which is

the positive tension in the cables [28]. A given pose belongs to WCW if it is able to generate positive cables tensions. However, WFW is defined by the maximum and the minimum of acceptable tensions, [29] [30].

The evaluation of parallel manipulators workspace remains an important research field. Discretization approaches presented in Fig. 4 have been widely used for workspace analysis [31]. The general principle consists of discretizing the 3-D space, calculate the inverse kinematic problem (IKP) at each point and check the constraints conditions. This method is easy to implement and can be applied to any robot type, however the computational time could be high, especially for robots with complex kinematic equations. Laribi *et al.* proposed an analytical method by determining the mathematical equations of the boundaries of the robot's workspace [14]. This method presented in Fig. 5 is based on the shape of the sub-workspace of each leg (or cable) of the robot. This formulation was used for several optimization problems [19], [32], [33].

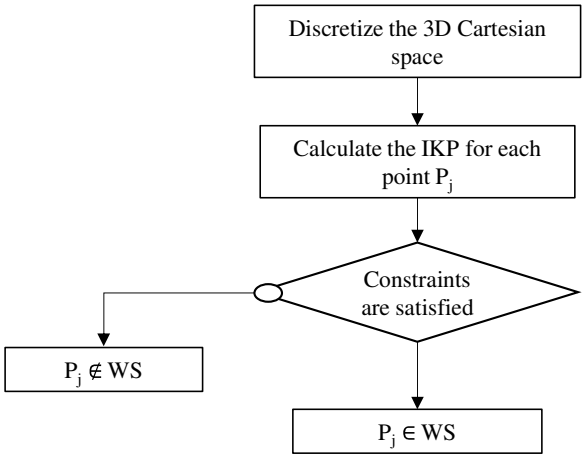

Fig. 4. Discretization Approach

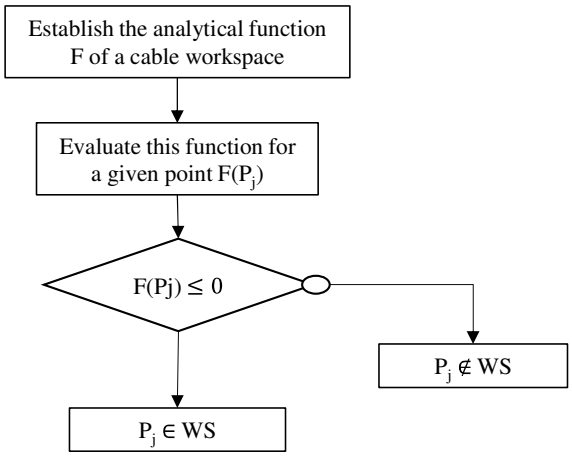

Fig. 5. Power point function Approach

4.2. Cables tensions

A cable can only pull on the attachment point due its flexible nature. This limitation adds an extra constraint when designing cable robots. Therefore, for the cable robot to function properly, the tensions in the different cables have to be maintained positive, at all times. In practice and to be on the safe side, the tension in any cable of the robot is always maintained greater than a non-zero minimum tension.

The optimization consists of minimizing the cables tensions values and consequently minimize the power consumption of the manipulator.

Under static conditions, the relation between cables' tensions and the wrench applied at the platform is given by Newton-Euler formulation.

$$\mathbf{W}\,\boldsymbol{\tau} = \mathbf{W_p} \tag{2}$$

Where

$\mathbf{W}$: is the structure matrix $(6 \times m)$

$\mathbf{W} = \begin{bmatrix} \mathbf{l_1} & \cdots & \mathbf{l_m} \\ \mathbf{l_1} \times \mathbf{p_1} & \cdots & \mathbf{l_m} \times \mathbf{p_m} \end{bmatrix}$; $\mathbf{l_i}$ is the vector of the i[th] cable direction and $\mathbf{p_i}$ is the vector from the *i*[th] attachment point to the inertia center of the end-effector.

$\boldsymbol{\tau} = [\tau_1 \ldots \tau_m]^T$ is the vector of all cables' tensions

$\mathbf{W_p} = [\mathbf{f}^T \ \mathbf{M}^T]^T$ is the external wrench applied on the end-effector.

In case of redundant actuation, the vector tension is given by the summation of the particular and homogeneous solutions as follows:

$$\boldsymbol{\tau} = \mathbf{W}^+ \mathbf{W_p} + (\mathbf{I}_m - \mathbf{W}^+\mathbf{W})\mathbf{s} \tag{3}$$

Where

$\mathbf{W^+}$**:** is the under-constrained Moore-Penrose pseudoinverse of $\mathbf{W}$.
$\mathbf{I_m}$: is the $m \times m$ identity matrix.
$\mathbf{s}$: is an arbitrary m-vector

$\bar{\boldsymbol{\tau}} = \mathbf{W}^+ \mathbf{W_p} = [\bar{\tau}_1 \dots \bar{\tau}_m]^{\boldsymbol{T}}$ is the particular solution however $\mathbf{Q} = (\mathbf{I_m} - \mathbf{W}^+\mathbf{W})\mathbf{s}$ is the homogeneous solution. To maintain positive tension on all cables, the homogeneous solution $\mathbf{Q}$ is fixed to guarantee a minimum required tension τ_{min} (see Fig. 6) [27].

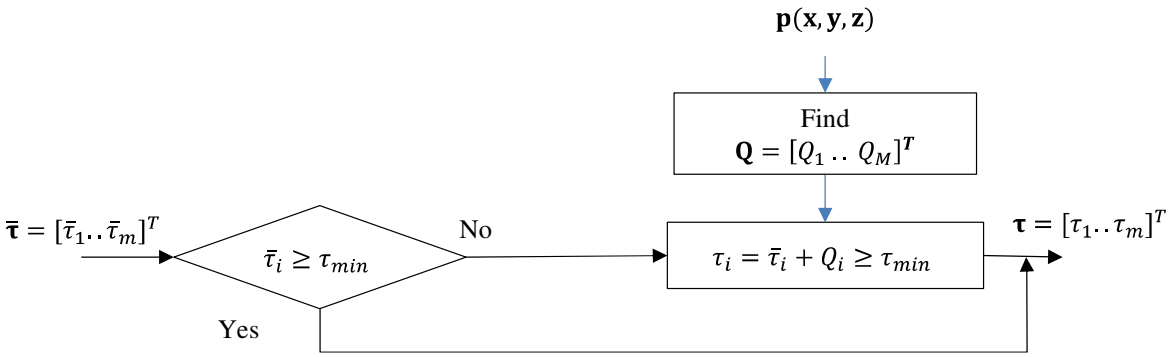

Fig. 6. Adjustable motor control

For mechanism synthesis problems, an objective function for the minimization of cable tensions was proposed in [19]. This function is expressed by:

$$F(\mathbf{I}) = \frac{1}{(\max(\boldsymbol{\tau}))^2}(\boldsymbol{\tau}^T.\boldsymbol{\tau}) \tag{4}$$

Where

$\boldsymbol{\tau} = [\tau_1, \tau_2, .., \tau_m]$, m is the number of cables of the manipulator
τ_i is the tension of the i^{th} cable

4.3. Cables sagging

In general, the studies on CDPRs consider the cables to be massless. However, in some cases with long-span cables, the aspect of sagging cables has to be taken into account. As shown in Fig. 7, a cable with a non-negligible mass has tendency to sag under its proper weight.
Cables sagging issue was addressed first by Jeong *et al.* [34] where an analytical expression of the longitudinal deformation of a cable was established and then a compensation factor of the cable deformation was proposed and validated through experimental tests.
Liu *et al.* [22] proposed a tension optimization approach for a cable driven parallel robot with large dimensions. The mathematical model for sagged cable layout proposed in [35] is used and then an iterative approach was applied to compute the cables tensions.

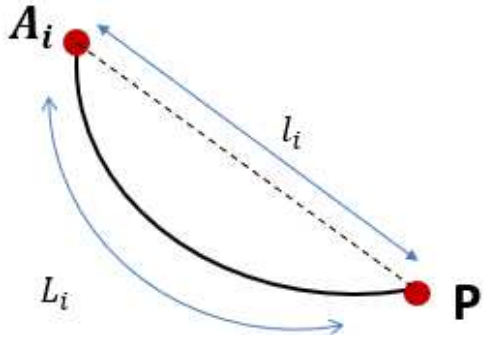

Fig. 7. Sagging cable in its vertical plane

4.4. Compactness

The compactness is a geometric criterion that characterizes the robot's size. There is no general formulation of this criterion. Essomba *et al.* [17] used the notion of local compactness function to optimize a spherical parallel manipulator. The index is given by the most inclined axis for a given configuration, then a global index is proposed through a discrete approach. For the same robot, Nelson *et al.* [36] proposed a compactness criterion as the sum of the angular design parameters. A different approach, proposed in [37], considers the robot's compactness as the ratio of a desired workspace by the entire volume occupied by the robot.
The calculation of the occupied volume by the robot depends on the base geometric shape, it could be a cube, a prism or a cylinder. Table 1 presents examples of different basic geometric shapes.

Table 1. Different bases shape

Robot		Occupied volume
LAWEX [19]	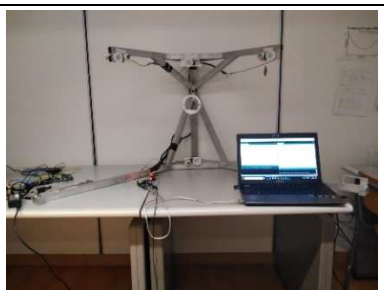	Cube $V = d^2 h$ Where d: is the horizontal position of the motors h: is the height of the robot
CUBE [9]	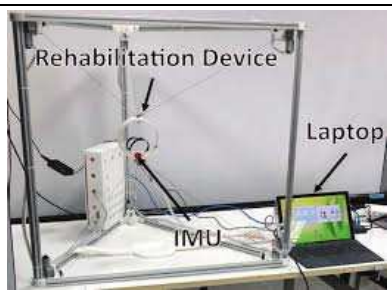	Prism $V = \frac{d^2}{2} h$ Where d: is the horizontal position of the motors h: is the height of the robot
FAST [2]		Cylinder $V = \pi R^2 h$ Where R: is the radius of the platform h: is the height

4.5. Singularity

Singular configurations correspond to the poses of the end-effector where the robots' performances degenerate and the control is lost. The determination of these configurations is essential in order to avoid them in the robot's trajectory. Generally, singularities can be identified through the examination of the Jacobian matrix. However, the Jacobian matrix considers all cables as rigid links. Therefore, the analysis of the Jacobian matrix becomes of no use if there is a slack in one of the robot's cable. Accordingly, two singularity cases can be distinguished [38]; the Jacobian singularity and force closure singularity, depending if the Jacobian matrix is singular or not and the force-closure condition is violated or not.
Recently, J-P Merlet [39] investigated the singularity of cable driven robots in case of sagging cables. In this case, the singularity analysis showed, in counter to rigid parallel robots, CDPRs present two class of singularities: inverse kinematic and forward kinematic singularities.

To describe the overall kinematic behavior of the robots, we use the error amplification factor, which is calculated using the inverse of the condition number $K(\mathbf{J})$, introduced by Gosselin [40].

$$\mu_j = \frac{1}{K(\mathbf{J})} \tag{5}$$

Where $K(\mathbf{J}) = \|\mathbf{J}\|.\|\mathbf{J}^{-1}\|$

J: is the Jacobian matrix of the robot at a given location

In the case of redundant actuation, the Jacobian matrix is a non-square matrix. The pseudo-inverse of the Jacobian matrix $\mathbf{J}^{+}$, is used instead of its inverse. The condition number can be understood as a measure of how sensitive the related function is to changes or errors in its entries. A large condition number also means that the matrix is getting close to being singular.

The condition number, in this case, is calculated as $K(\mathbf{J}) = \|\mathbf{J}\|.\|\mathbf{J}^{+}\|$

To evaluate the global dexterity within the desired workspace, a global conditioning index ranging between 0 and 1 is defined in Eq. (6)

$$\mu = \frac{\sum_{j=1}^{N} \mu_j}{N} \tag{6}$$

Where N is the discretization parameter of the desired workspace. The best kinematic performance is reached when μ= 1
The use of the condition number is not appropriate for manipulators having translational and rotational DOF and the normalization of the Jacobian matrix will be needed.

4.6. Safety

Safety issues are of a great importance in the design of robotic devices. The human-robot interaction has been investigated in several works mainly for medical devices, where the user is in direct physical contact with the manipulator. The increase of use of medical robots, requires the definition of specific safety standards since the safety measures of medical and industrial robots should be different.
The « IEC 80601-2-78:2019» is a recent ISO standard applies to the general requirements for basic safety and essential performance of medical robots that physically interact with a patient with an impairment to support or perform rehabilitation, assessment, compensation or alleviation [41]. Since the workspace in these situations is shared by the robot and the patient, conventional measures requiring a safety zone cannot be applied. The « IEC 80601-2-78:2019» standards evokes the risk management and situation awareness due to mechanical and electrical hazards. Different situations have been tackled as Energy release, exceeding the patient's movement limits, misalignment and collisions.
Carbone *et al.* [42] have highlighted 3 aspects that affect patient's safety during a rehabilitation task:

- Operation ranges: when the robot moves the patient limb outside its operation space.
- Operation modes: when the robot speed is greater than the patient safe speed.
- Operation forces/torques: when the robot exercises an important effort on the human limb.

To ensure that the robot's works on a safety mode, the knowledge of the human operation ranges, modes and forces is required.
Another safety measure has been investigated in literature, which is the detection of cable failure. In fact, an emergency stop is often used with classical rigid robots however due to the flexibility of cables, the braking of motors could be not enough to stop the robot. Boschetti *et al.* [43] proposed an operational strategy for cable failure that consists in generating an opposite wrench in case of failure, which leads the end-effector to a safe position.

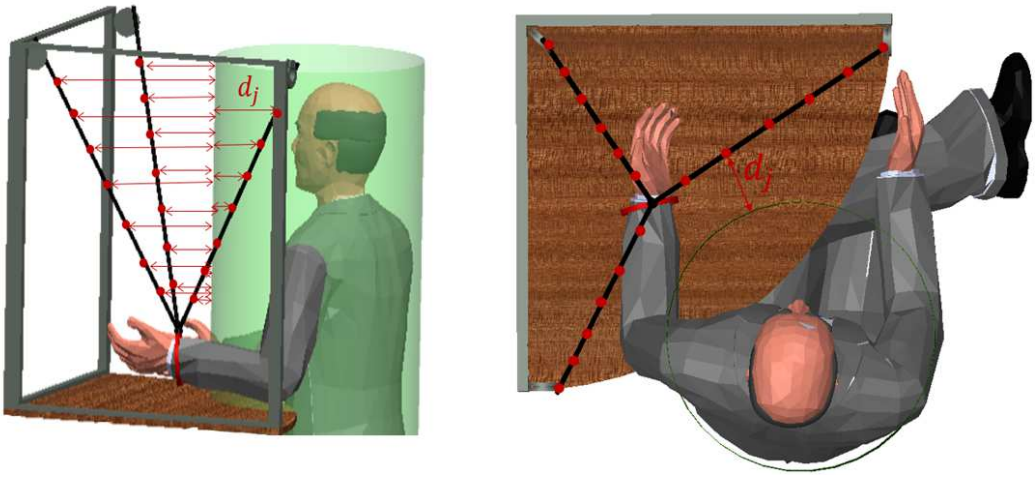

Fig. 8. Safety criterion

Another criterion that have been introduced in a previous work [44] is the minimum distance between the cables and the patient during the rehabilitation task as presented in Fig. 8. The approach consists in discretizing the cables' line into *t* points and calculate the distance between each point and the cylinder surrounding the patient. The cylinder surrounding the patient with diameter D, the shoulder width, and centered on its spine is presented in Fig 9. The objective of this method is to maximize this distance to avoid any risk of collision between the user and the robot. The distance d_j between a given point $P_j\ (x_j, y_j, z_j)$ on the cable and the cylinder, the safety area of the patient, is given by the following equation.

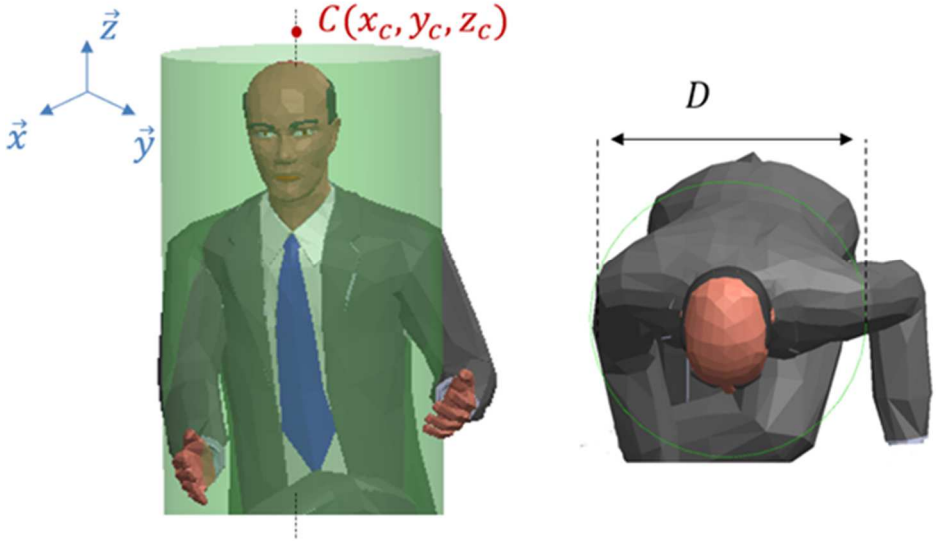

Fig. 9. Dimension and position of the cylinder surrounding the patient

$$d_j = \sqrt{(x_j - x_c)^2 + (y_j - y_c)^2} - \frac{D}{2} \tag{7}$$

Where x_c, y_c, z_c are the coordinates of a point from the cylinder axis ($z_c = z_j$).

4.7. Overview

Table 2 presents an overview of the presented criteria. As it can be seen, some of them could be considered as constraints or/and objectives.

Table 2. Summary of the CDPR criteria

	Constraint	Performance
Workspace	✔	✔
Compactness	x	✔
Dexterity	x	✔
Singularity	✔	x
Payload and weight	✔	✔
Cables tensions	✔	✔
Safety	✔	✔
Cables interferences	✔	x
Cables sagging	✔	x
Power consumption	✔	✔

5. A Case of Study

5.1. Requirements and constraints for forearm rehabilitation tasks

CDPRs achieved interesting results regarding physical rehabilitation of post-stroke patients. Among the physiotherapy exercises for post stroke patients is the Elbow flexion/extension planar movement shown in Fig. 10 [42], [45], [46]. It consists of an arc of center the elbow of the patient and radius the length of the forearm. To define the workspace required for this particular exercise several measures of 10 normal subjects of different ages (25 – 70 years) and gender, have been carried out. The results are given in Table 3. According to the obtained movements ranges, a desired workspace, presented in Fig. 11, was defined as a surface limited by two arcs corresponding to the maximal and minimum forearm lengths.

Table 3. Elbow mouvement mesures

	Forearm length (cm)	Lower limit (°)	Upper limit (°)
1	27	0	125
2	21	0	130
3	30	5	150
4	27	0	130
5	25	0	120
6	32	0	125
7	30	0	140
8	23	5	135
9	28	0	150
10	31	0	130

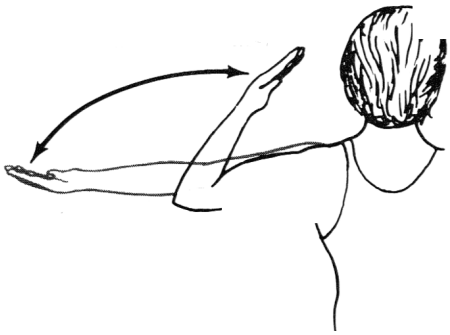

Fig. 10. Flexion movement of upper arm

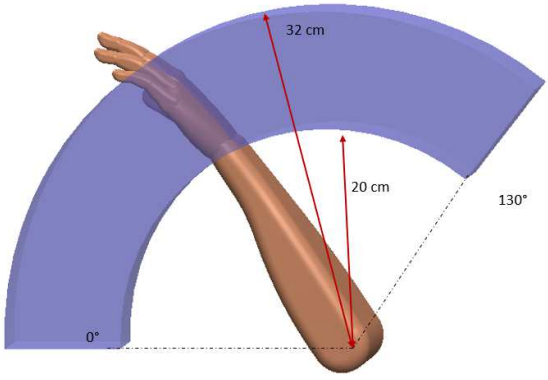

Fig. 11. Desired workspace

LAWEX robot, shown in Fig. 12, is a rehabilitation device built in LARM in Cassino [42]. It consists of 4 motors controlling the lengths of 4 flexible cables attached to a circular end-effector. The used

cables are thin with negligible weights so that sagging issue can be considered as negligible. As a rehabilitation device, LAWEX operates at low speed. The weight of the moving part is estimated to be equal to 1.5 Kg, including the average weight of a human hand and forearm, as it is reported in [47].

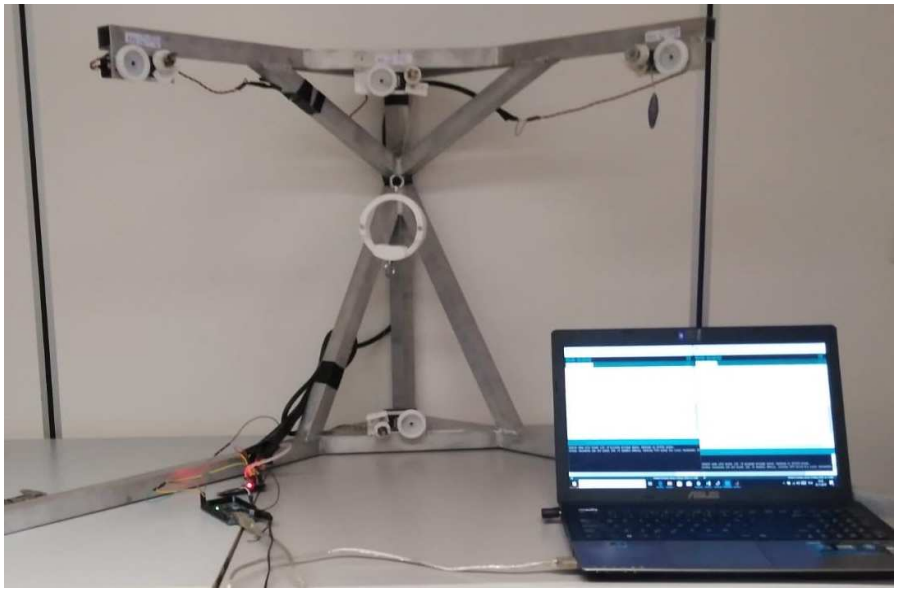

Fig. 12. LAWEX robot

This section aims at the study and the comparison of four different designs of LAWEX robot (see Fig. 13). The objective is to select the optimal design and the optimal parameters of the robot having the *best* tension distribution along the prescribed trajectory and occupying the smallest volume.

By assuming that the orientation of the end-effector during the rehabilitation task is constrained, we consider only the forces generated by the cables' tensions and the moments are neglected.

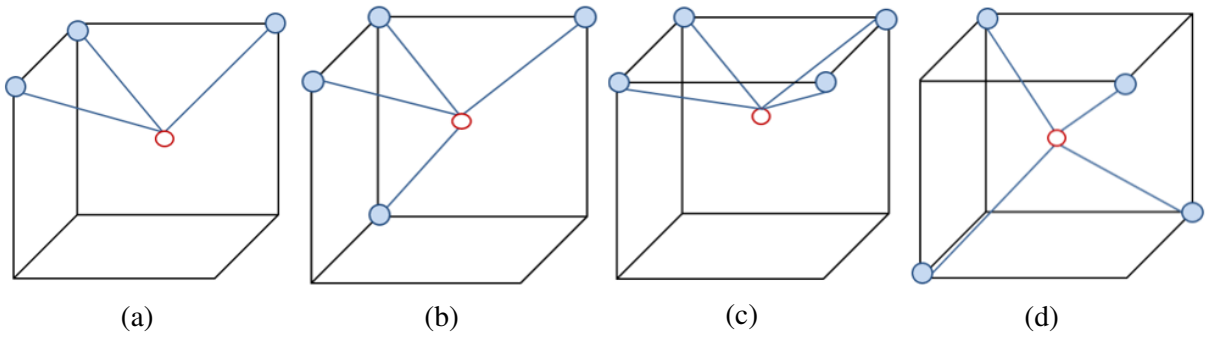

Fig. 13. Different designs of LAWEX robot: (a) Under-constrained suspended CDPR (b) Fully constrained CDPR (c) under-constrained suspended CDPR and (d) Fully constrained CDPR

5.2. Geometric and kinematic modellings for different topologies

5.2.1. Design (a), Under-constrained suspended CDPR

This design consists of a suspended cable driven robot with 3 cables attached in the same point of the end-effector. The inverse geometric model of a cable driven parallel robot defines the lengths of cables according to the end-effector position. The position of the end effector is given by the vector $\mathbf{p} = [x, y, z]^T$.

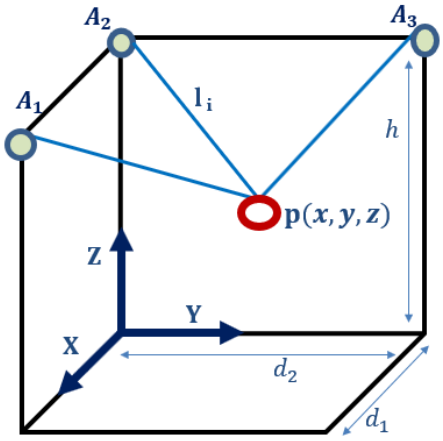

Fig. 14. Geometric Parameters of design (a)

The motors positions according to Fig. 14 are given by the following equations.

$$\begin{aligned} \mathbf{A_1} &= [d_1, 0, h]^T \\ \mathbf{A_2} &= [0\ , 0\ , h]^T \\ \mathbf{A_3} &= [0, d_2, h]^T \end{aligned} \tag{8}$$

The inverse kinematic model (IKM) is obtained by the closed-loop equation of each cable defined in the following equation.

$$\mathbf{p} = \mathbf{A_1} + \mathbf{l_1} = \mathbf{A_2} + \mathbf{l_2} = \mathbf{A_3} + \mathbf{l_3} \tag{9}$$

here

$\mathbf{l_i}$: is the vector from the i^{th} motor to the end-effector.

x, y, z: are the coordinates of the end-effector.

$$\begin{cases} \mathbf{l_1} = \mathbf{p} - \mathbf{A_1} \\ \mathbf{l_2} = \mathbf{p} - \mathbf{A_2} \\ \mathbf{l_3} = \mathbf{p} - \mathbf{A_3} \end{cases} \tag{10}$$

The IKM is given by the length of the 3 cables

$$\begin{cases} l_1 = \|\mathbf{p} - \mathbf{A_1}\| = \sqrt{(x-d_1)^2 + y^2 + (z-h)^2} \\ l_2 = \|\mathbf{p} - \mathbf{A_2}\| = \sqrt{x^2 + y^2 + (z-h)^2} \\ l_3 = \|\mathbf{p} - \mathbf{A_3}\| = \sqrt{x^2 + (y-d_2)^2 + (z-h)^2} \end{cases} \tag{11}$$

$$\begin{pmatrix} l_1 \\ l_2 \\ l_3 \end{pmatrix} = \begin{pmatrix} \sqrt{(x-d_1)^2 + y^2 + (z-h)^2} \\ \sqrt{x^2 + y^2 + (z-h)^2} \\ \sqrt{x^2 + (y-d_2)^2 + (z-h)^2} \end{pmatrix} \tag{12}$$

The cables tensions are given by the Newton Euler formulation as follows

$$\mathbf{W}\,\boldsymbol{\tau} = \mathbf{W_p} \tag{13}$$

Where

$\boldsymbol{\tau} = [\tau_1, \tau_2, \tau_3]^T$

$\mathbf{W_p} = [0\ \ 0\ \ -M_a g\ ]^T$, M_a: end-effector mass, g: gravitational acceleration

$\mathbf{W} = [W_1, W_2, W_3]$, $\boldsymbol{W_i} = \begin{bmatrix} \mathbf{U_i} \\ \mathbf{p_i} \times \mathbf{U_i} \end{bmatrix}$, $\mathrm{U_i} = -\mathbf{l_i}/l_i$

$\mathbf{p_i}$: is the vector connecting the reference point on the moving platform $\mathbf{p}$ to the anchor point of the i^{th} cable**.**

The Jacobian Matrix of the LAWEX robot is given by

$$\mathbf{J} = \mathbf{W}^{\mathrm{T}} = \begin{pmatrix} \frac{x-d_1}{l_1} & \frac{y}{l_1} & \frac{z-h}{l_1} \\ \frac{x}{l_2} & \frac{y}{l_2} & \frac{z-h}{l_2} \\ \frac{x}{l_3} & \frac{y-d_2}{l_3} & \frac{z-h}{l_3} \end{pmatrix} \tag{14}$$

5.2.2. Design (b), fully constrained CDPR

For this design, four cables are used to control the end-effector pose. However, we consider the orientation of the end-effector to be constrained due to a fixed support of the patient elbow. In this case, the LAWEX robot is a fully constrained mechanism where the end-effector position is defined by the length of the 4 cables. The considered parameters are given in Fig. 15.

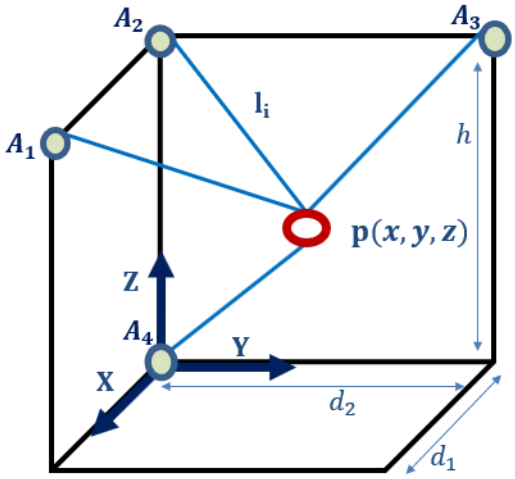

Fig. 15. Geometric Parameters of Design (b)

The IKM of the fully constrained CDPR is given by Eq (15).

$$\begin{pmatrix} l_1 \\ l_2 \\ l_3 \\ l_4 \end{pmatrix} = \begin{pmatrix} \sqrt{(x-d_1)^2 + y^2 + (z-h)^2} \\ \sqrt{x^2 + y^2 + (z-h)^2} \\ \sqrt{x^2 + (y-d_2)^2 + (z-h)^2} \\ \sqrt{x^2 + y^2 + z^2} \end{pmatrix} \tag{15}$$

The cables tensions are obtained, as in the previous case, through Newton-Euler formulation.

$$\mathbf{W}\,\boldsymbol{\tau} = \mathbf{W_p} \tag{16}$$

where

$\boldsymbol{\tau} = [\tau_1, \tau_2, \tau_3, \tau_4]^T$

$\mathbf{W_p} = [0 \;\; 0 \;\; -M_a g \;]^T$, M_a: end-effector mass, g: gravitational acceleration

$\mathbf{W} = [W_1, W_2, W_3, W_4]$, $\mathbf{W_i} = \begin{bmatrix} \mathbf{U_i} \\ \mathbf{p_i} \times \mathbf{U_i} \end{bmatrix}$, $\mathbf{U_i} = -\mathbf{l_i}/l_i$

Since the mechanism is over constrained, there is an infinite number of solutions of the tension vector. The vector tension is given by the following equation.

$$\boldsymbol{\tau} = \bar{\boldsymbol{\tau}} + \beta\,\mathbf{N} \tag{17}$$

where

$\bar{\boldsymbol{\tau}} = \mathbf{W}^{+}\mathbf{W}_{p}$: is the particular solution of Eq (19) where $\mathbf{W}^{+}$ is the Moore-Penrose pseudoinverse of $\mathbf{W}$

$\mathbf{N}$: is the Kernel vector of $\mathbf{W}$

β: is an arbitrary scalar chosen so that τ_i $(i = 1..4)$ is greater than the minimum desired tension.

In our case, we fix $\tau_{min} = 0.5$ N. The value of 0.5 N has been selected by referring to the maximum loading conditions of LAWEX (1.5 Kg) and to the mass of the LAWEX cables (nylon cables, whose weight is about 5 grams per meter). Accordingly, a ten times higher cable tension value provides a negligible sagging effect. This assumption is also discussed in [43].

5.2.3. Design (c), under constrained suspended CDPR

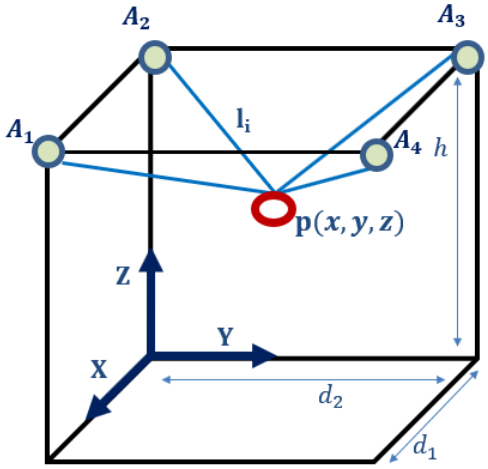

Fig. 16. Geometric parameters of design (c)

For this design, four cables are used to control the end-effector pose. In this case, the LAWEX robot is a redundant mechanism where the end-effector position is defined by the length of the 4 cables. The considered parameters are given in Fig. 16.

The IKM of the over constrained CDPR is given by Eq (18).

$$\begin{pmatrix} l_1 \\ l_2 \\ l_3 \\ l_4 \end{pmatrix} = \begin{pmatrix} \sqrt{(x-d_1)^2 + y^2 + (z-h)^2} \\ \sqrt{x^2 + y^2 + (z-h)^2} \\ \sqrt{x^2 + (y-d_2)^2 + (z-h)^2} \\ \sqrt{(x-d_1)^2 + (y-d_2)^2 + (z-h)^2} \end{pmatrix} \tag{18}$$

Cables tensions are given through the Newton Euler formulation (Eq (19))

$$\mathbf{W}\,\boldsymbol{\tau} = \mathbf{W}_{p} \tag{19}$$

Where

$\boldsymbol{\tau} = [\tau_1, \tau_2, \tau_3, \tau_4]^T$

$\mathbf{W_p} = [0 \;\; 0 \;\; -M_a g \;]^T$, M_a: end-effector mass, g: gravitational acceleration

$\mathbf{W} = [W_1, W_2, W_3, W_4\,]$, $\mathbf{W_i} = \begin{bmatrix} \mathbf{U_i} \\ \mathbf{p_i} \times \mathbf{U_i} \end{bmatrix}$, $\mathbf{U_i} = -\mathbf{l_i}/l_i$

The tension vector is obtained by summation of the particular and a homogeneous solution as defined in Eq (17) of the previous case.

5.2.4. Design (d), fully constrained CDPR

In this design, four cables are distributed above and below the platform as shown in Fig. 17. The motors positions are given in the following Equations:

$$\mathbf{A_1} = [0, 0, h]^T$$
$$\mathbf{A_2} = [d_2\ , d_2\ , h]^T$$
$$\mathbf{A_3} = [d_1, 0, 0]^T$$
$$\mathbf{A_4} = [0, d_2, 0]^T$$

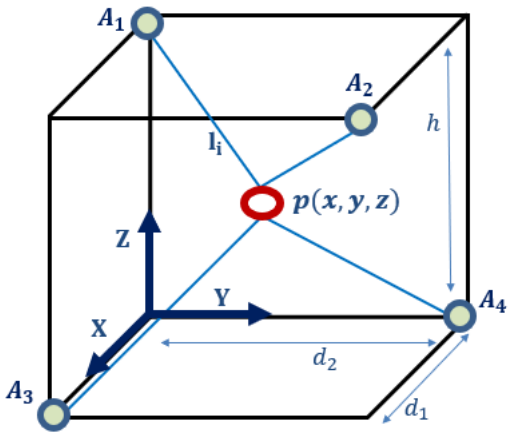

Fig. 17. Geometric Parameters of design (d)

The IKM of the fully constrained CDPR is given by Eq.(**20**)

$$\begin{pmatrix} l_1 \\ l_2 \\ l_3 \\ l_4 \end{pmatrix} = \begin{pmatrix} \sqrt{x^2 + y^2 + (z-h)^2} \\ \sqrt{(x-d_1)^2 + (y-d_2)^2 + (z-h)^2} \\ \sqrt{(x-d_1)^2 + y^2 + z^2} \\ \sqrt{x^2 + (y-d_2)^2 + z^2} \end{pmatrix} \tag{20}$$

The cables tensions are obtained through Newton-Euler formulation and the solution is defined as in the previous two cases

5.3. Mathematical formulation of the optimization problem

The objective of this optimization is to select the best LAWEX design (a , b, c, or d) and the best set of design parameters that guarantee the best compromise between cables tension and the compactness criterion for a prescribed rehabilitation trajectory.

Given:

- Trajectory of the patient wrist

Objectives:

- Include the prescribed trajectory;
- Minimize the occupied volume by the robot;
- Minimize the maximum cables tensions.

A mathematical formulation of the optimization problem is given as follows:

$$\begin{cases} \text{Minimize } F(\mathbf{I}) = \begin{cases} F_1(\mathbf{I}) \\ F_2(\mathbf{I}) \end{cases} \\ \text{Subject to } C_i(\mathbf{I}) \leq 0 \\ \mathbf{I} = [x_1, .., x_n] \\ x_{j\,min} < x_j < x_{j\,max} \end{cases} \tag{21}$$

where

$F_1(\mathbf{I})$ and $F_2(\mathbf{I})$ are the objective functions defining the robot's size and the cables tensions, respectively.
$C_i(\mathbf{I})$ are the constraint functions describing the prescribed trajectory.
$\mathbf{I} = [x_1, .., x_n]$ is the decision vector defined by the set of design variables and $x_{j\,min}$, $x_{j\,max}$ the search domain for each design variable x_j.

5.3.1. The proposed solving algorithm approach

A novel approach for mechanism synthesis is proposed in Fig. 18. It aims to expand the Non-dominated Sorting Genetic Algorithm (NSGA-II) [48] allowing the synthesis of more than one architecture.

The NSGA-II optimization algorithm is an evolutionary elitist algorithm inspired from the natural evolutionary process. The strength of this metaheuristic is highlighted especially with complex problems involving several objectives and/or constraints.

Two types of coding, discrete and real, can be used to represent individuals (solutions) of the Genetic Algorithm. The Main contribution of this approach is to combine both coding types in the same formulation. The design vector is composed of two parts: a discrete part handling the design type and a continuous part handling the set of design parameters of the studied manipulator.

Starting for a randomly generated initial population, the individuals are evaluated, selected and then genetical operators are applied (Crossover and mutation).

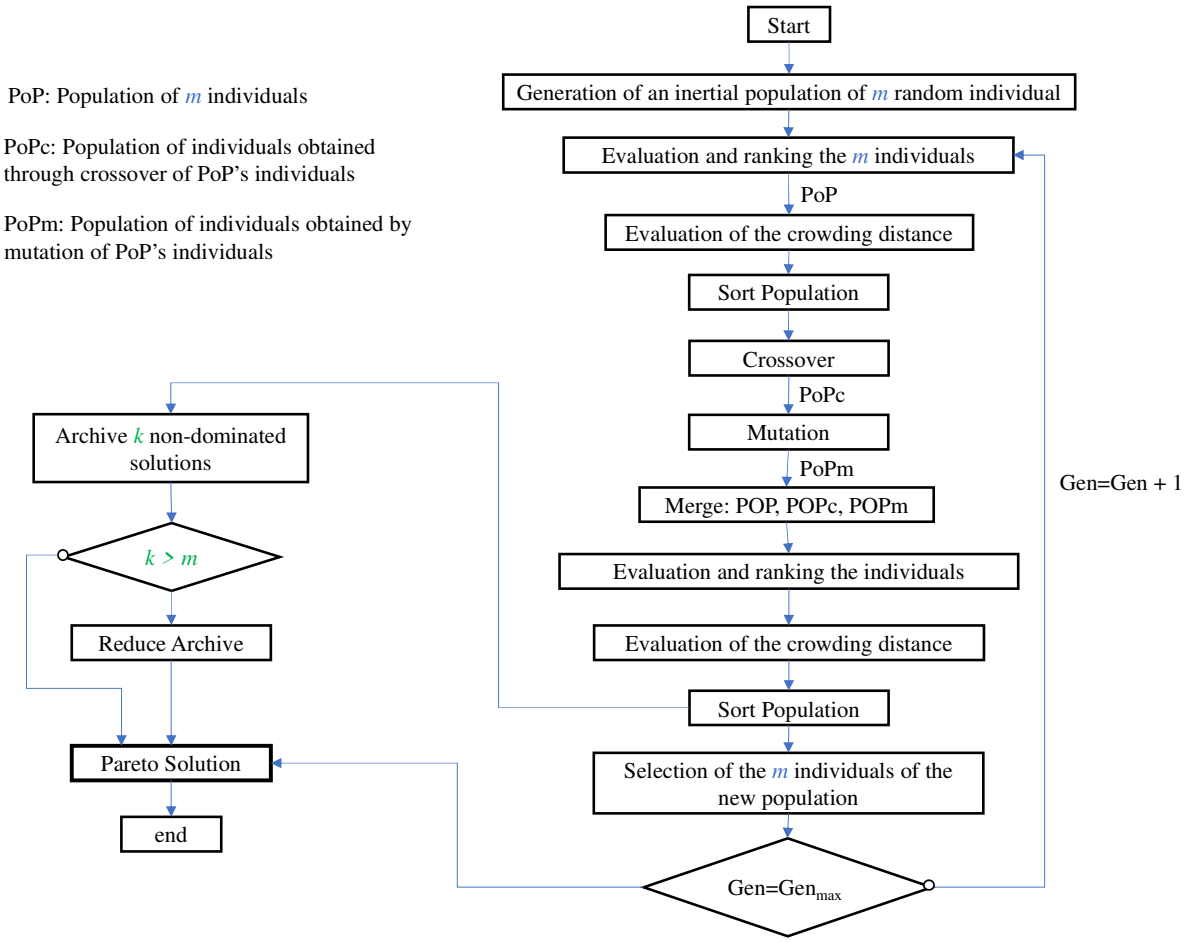

Fig. 18. Flow chart of the proposed approach

The initial population is created randomly with an arbitrary number of each design type then evaluation, ranking and sort of the individuals according to the crowding distance, are performed. After combination of the old population and the new individuals obtained through crossover and mutation operators, the set is raked and sorted according to the crowding distance. A new generation is

born by applying selection operator. From each generation, a parallel selection is made to select the non-dominated solutions which will appear in the Pareto front. The same steps are repeated with new generations until achieving one of the stopping criteria. The considered stopping criterion is the maximum number of generations.

5.3.2. The decision vector

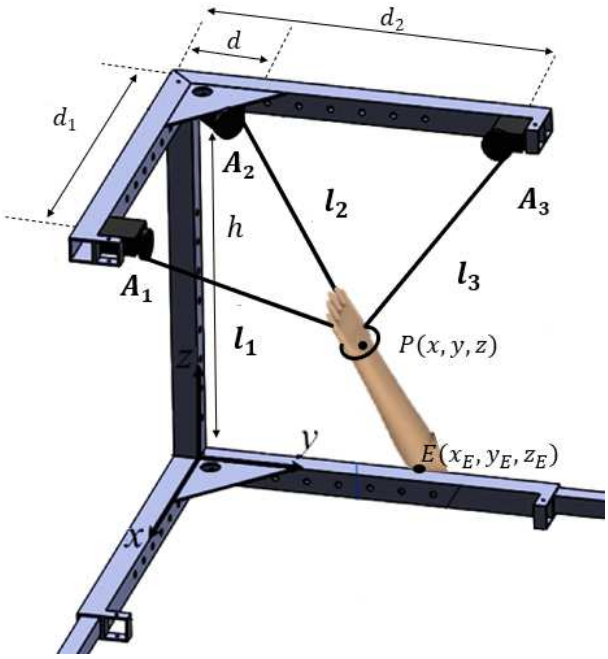

Fig. 19. Design parameters of the design approach

The decision vector of the proposed approach is composed of two parts, a discreate variable ($des = 1,2,3,4$) referring to the selected design *a, b, c* or *d* and a design vector composed of continuous design parameters of the robot. The decision vector is given by:

$$\mathbf{I} = [des, d_1, d_2, h, r, z_E]^T \tag{22}$$

where: $des = 1, 2, 3,4$: assigns the design type (see Fig. 13)
d_1, d_2, h : design parameters of the robot
$r = x_E\sqrt{2} = y_E\sqrt{2}$
x_E, y_E, z_E: position of the patient elbow as shown in Fig. 19**.**

5.3.3. The selected objective functions

- **Compactness**

This criterion aims to reduce the occupied volume by the robot. It is computed as the ratio of the cuboid robot's volume by the volume of the actual design (see Fig. 12).

$$F_1(I) = \frac{d_1 \times d_2 \times h}{V_{LAWEX}} \tag{23}$$

Where V_{LAWEX}: is the volume of the built prototype at LARM Cassino. The design parameters of this prototype are given in Table 4.

Table 4 : Design parameters of LARM Prototype

$d_{1\,LAWEX}$	$d_{2\,LAWEX}$	$h_{\,LAWEX}$	V_{LAWEX}
0.6 m	0.6 m	0.65 m	0.234 m^3

- **Cables tensions**

To guarantee a minimal cables tension along the prescribed trajectory, the objective function is given as a ratio of the calculated maximal tension at a point from the trajectory by the maximal tension of the existing prototype

$$F_2(I) = \frac{\max(\boldsymbol{\tau})}{\tau_{max}} \tag{24}$$

5.3.4. The defined constraint functions

The proposed optimization problem is subject to two constraints:

- The belonging of the desired trajectory to the robot workspace
- A positive cables' tension

To examine if a given point (x, y, z) from the trajectory is inside the workspace or not, the power point function is used as follows:

$$\begin{cases} f_{i\,max} = (x - x_{Ai})^2 + \left(y - y_{Ai}\right)^2 + (z - z_{Ai})^2 - {l_{max}}^2 \leq 0 \\ f_{i\,min} = {l_{min}}^2 - (x - x_{Ai})^2 + \left(y - y_{Ai}\right)^2 + (z - z_{Ai})^2 \leq 0 \end{cases}, i = 1,2,3 \tag{25}$$

To ensure a positive cables tension, the Moore–Penrose inverse, presented in section 4.2, is used

$$\boldsymbol{\tau} = \bar{\boldsymbol{\tau}} + \boldsymbol{Q} \geq 0 \tag{26}$$

where

$\bar{\boldsymbol{\tau}} = \mathbf{W}^+ \mathbf{W_p}$, $\mathbf{W}^+$**:** is the under-constrained Moore-Penrose pseudoinverse of $\mathbf{W}$.

$\mathbf{Q} = (\mathbf{I_m} - \mathbf{W}^+\mathbf{W})\mathbf{s}$, $\mathbf{I_m}$: is the $m \times m$ identity matrix, $\mathbf{s}$: is an arbitrary m-vector

A penality function is considered to ensure that the problem constraints are respected and it is given as bellows:

$$F_0(I) = \begin{cases} 0 & if\ constraints\ are\ satisfied \\ cf & otherwise \end{cases} \tag{27}$$

Here, cf is a large positive constant.

5.4. Numerical implementation and results

The described optimization problem is solved using MATLAB software. The modified NSGA-II algorithm was implemented with the following inputs: population size = 500, and number of generations =100.

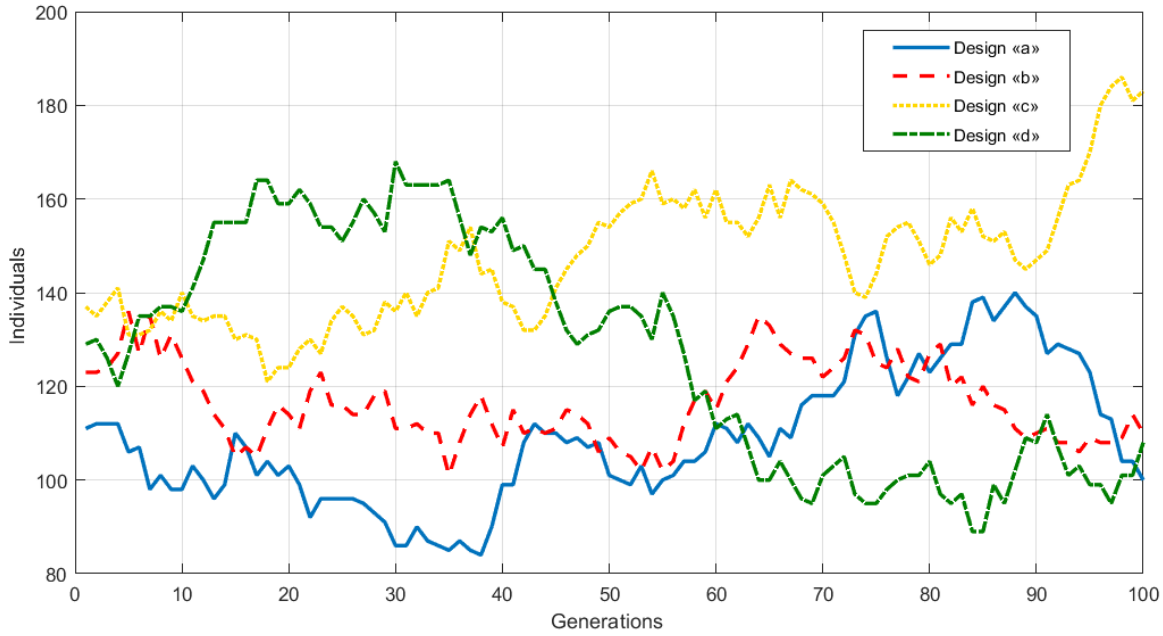

Fig. 20. Evolution of solutions type through generations

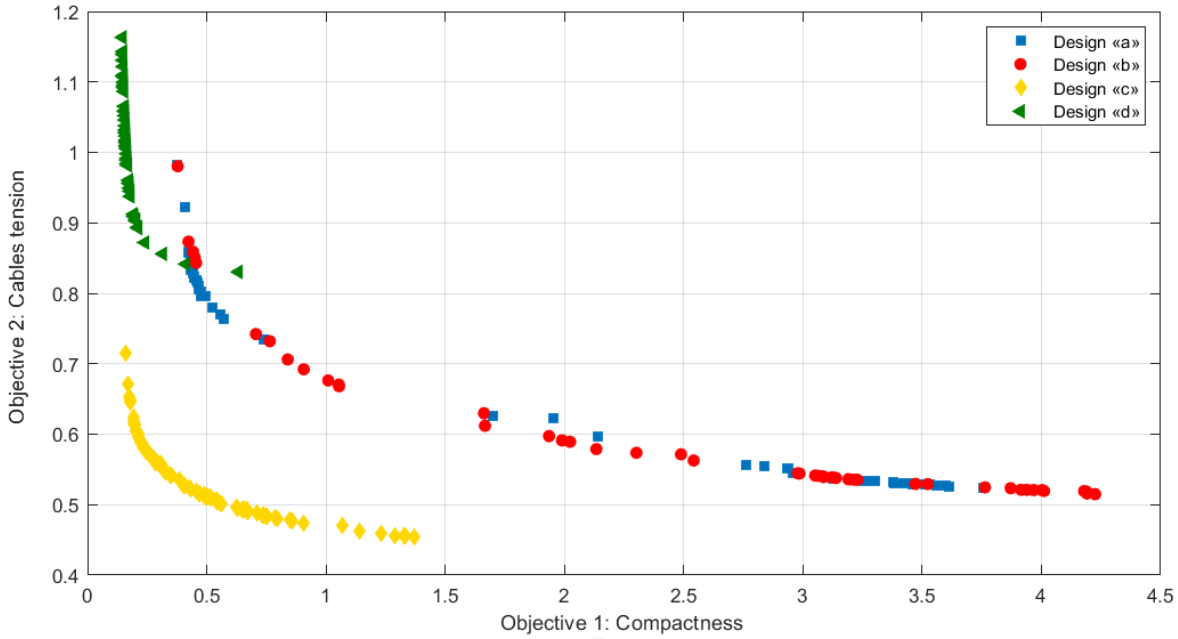

Fig. 21. Last population solutions

Fig. 20 gives the evolution of the different robot's designs from one population to another. To assure the transition of the four designs from generation to generation, a minimum ratio of $p = 10\%$ individuals from the population size of each design is imposed. The evolution of populations shows that starting from the 50^{th} generation, designs «c» starts taking advantage and dominates the population individuals.

To analyze the dominance of «c» Individuals, a presentation of the last generations in terms of the objective function is given in Fig. 21. The solutions of design «c» are numerous but very close; they have close fitness values however, the solutions of designs «a» and «b» are more scattered.

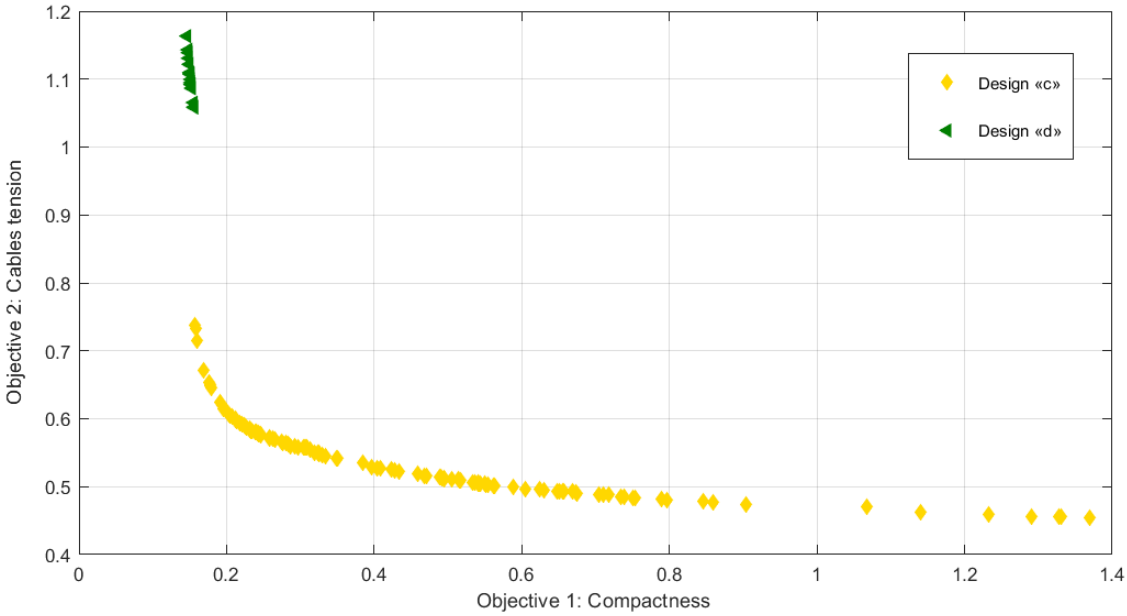

Fig. 22. Pareto front

Fig. 22 presents the set of non-dominated optimal solutions called Pareto front of the optimization process. The first and second designs, «a» and «b», are excluded from the Pareto front since their solutions are dominated solutions. The minimum cables tension is obtained for the third design «c» where the end-effector is suspended by four cables while the best compactness values are presented by design «d», where the cables are fairly distributed below and above the end-effector. We called this design 2-2 topology.

The solutions having a compactness index greater than 1 in the Pareto front are the solutions with a bulkier design than LARM prototype.

Discontinuity of the Pareto front along cables tension index axis can be explained by heterogeneity of the studied designs where the compactness index is a common function of all designs and cables tension function is specific for each design. To examine the point of discontinuity, both solutions of the gap point of the Pareto front are identified (Table 5) and presented in Fig. 23.

Fig. 23 shows that the occupied volume of both solutions is very close however a considerable difference of the maximal cable tension is recorded along the desired trajectory. The distinction of motors position from a design to another affects the static equilibrium of the end-effector and then the applied efforts.

Table 5. Two selected solutions from the Pareto front

	Design	d_1	d_2	h	r	z_e
I	4	0.3 m	0.3 m	0.404 m	0.281 m	0.05 m
	3	0.3 m	0.302 m	0.405 m	0.281 m	0.05 m

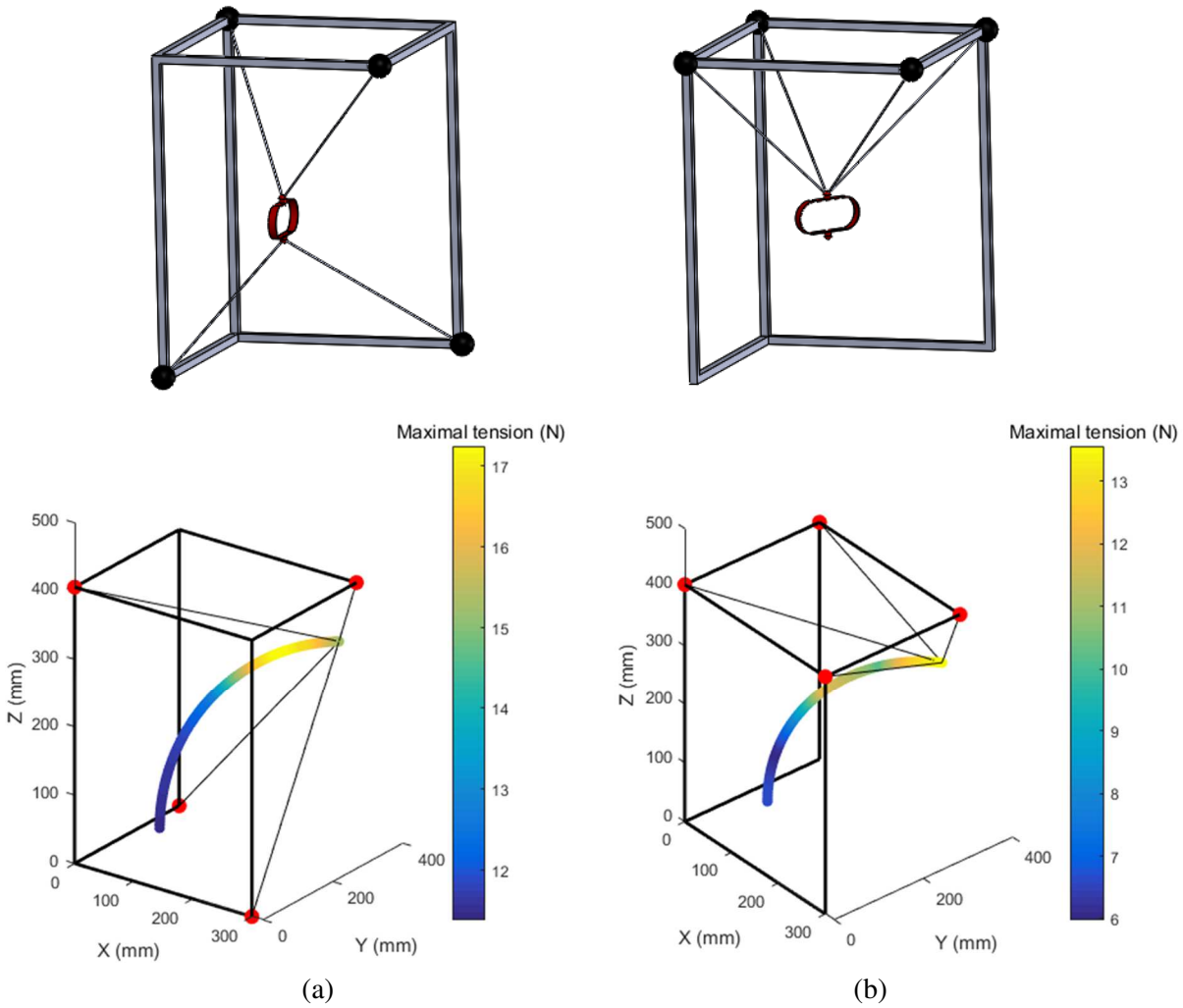

(a) (b)

Fig. 23. CAD and maximal tension distribution of the two selected solutions from the Pareto front

5.4.1. Pareto front selection approach

To select a single solution from the set of the Pareto front, a novel criterion is proposed. The decision process is performed relatively to the patient safety. We consider the approach presented previously in Fig. 8. It consists in evaluating the minimum distance between the cables and the user, nb points are selected on each cable at equal distance and then the distance from a point p_{ij} to the patient is calculated where $i = 1..m$ and $j = 1..nb$. To simplify the model, we consider the axis centered on the spine of the patient. To evaluate patient safety, the minimum distance between cables and the patient is computed.

$$F_s = min\,(P_{ij}) \tag{28}$$

Where $P_{ij} = \sqrt{(x_{ij} - x_c)^2 + (y_{ij} - y_c)^2} - \frac{D}{2}$ is the distance from the point p_{ij} to the cylinder

x_{ij}, y_{ij} : are the coordinates of the point p_{ij}

The safety function is computed for all Pareto solutions. The ranking of Pareto solutions reveals that the design «d» is safer for the patient than solutions of design «c» with a minimum distance equal to 10cm during desired trajectory. The solution which guarantee the maximal distance between cables and patient is selected. Design parameters of this solution are given in Table 6.

Results show that a 2-2 topology is the best topology for the selected optimality criteria. Also, the dimensional synthesis provide feasible sizes for fulfilling the desired design requirements in terms of optimal tradeoff between occupied robot volume, cable tensions and the user safety.

Table 6 : Design parameters of the selected solution

	Design	d_1	d_2	h	r	z_e
I	4	0.3 m	0.3 m	0.386 m	0.284 m	0.053 m

5.4.2. Comparison of the obtained solutions with the LAWEX prototype

Design parameters of the existing LAWEX rehabilitation device (Fig. 12) are given in Table 7.

Table 7. Design parameters of the existing LAWEX prototype

	$d_{1\ LAWEX}$	$d_{2\ LAWEX}$	h_{LAWEX}	r_{LAWEX}	$z_{E\ LAWEX}$
$\mathbf{I}_{\mathbf{LAWEX}}$	0.6 m	0.6 m	0.65 m	0.29 m	0.22 m

The index of cables tension on the Pareto front of design «d» solutions is greater than 1 which attested a maximal cables tension slightly greater than LAWEX prototype maximal cables tension. Fig. 24 shows a difference going from 2 to 4 N along the prescribed trajectory between both designs.

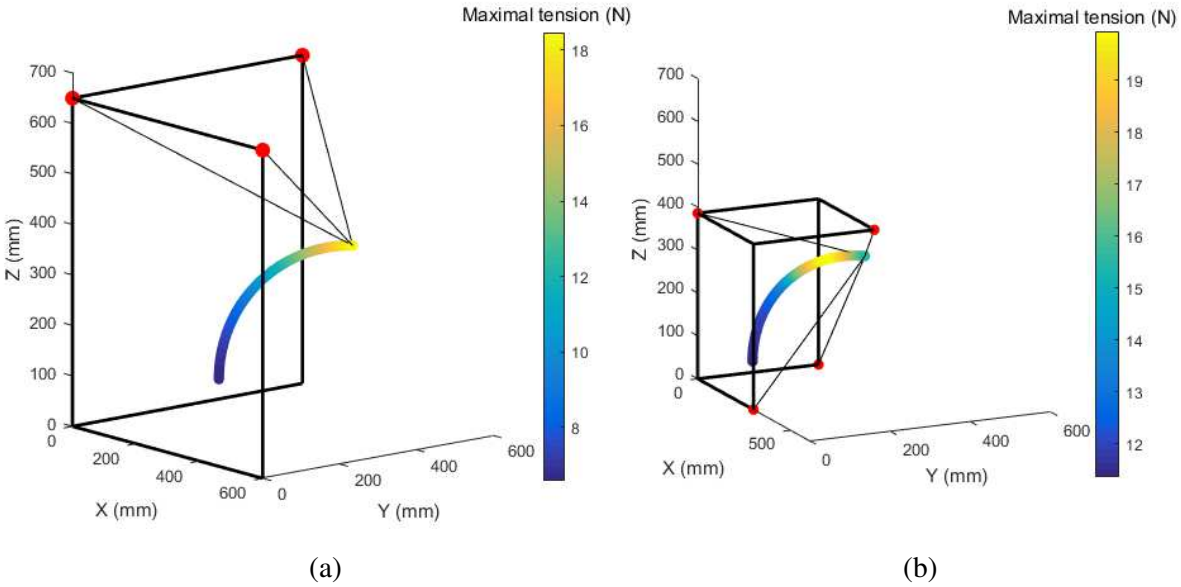

(a) (b)

Fig. 24. Maximal cables tension of LAWEX prototype in N: (a) LAWEX prototype, (b) selected optimal solution

Fig. 25 presents the CAD models of LAWEX prototype and the selected solution. A significant difference on the occupied volume by both designs can be noticed. An evaluation of the occupied volume and maximal cables tension are given in Table 8. Results demonstrate a 2-2 topology as being the most effective in terms of the selected optimality criteria with optimal tradeoff between occupied robot volume, cable tensions and the user safety. Namely, it has been possible to achieve a reduction of the occupied volume of about 85% while maximum cable tension has been reduced by 2%. In terms of safety, the actual prototype is still 38% safer than the selected solution due to the position of exiting points which are secluded from the patient position.

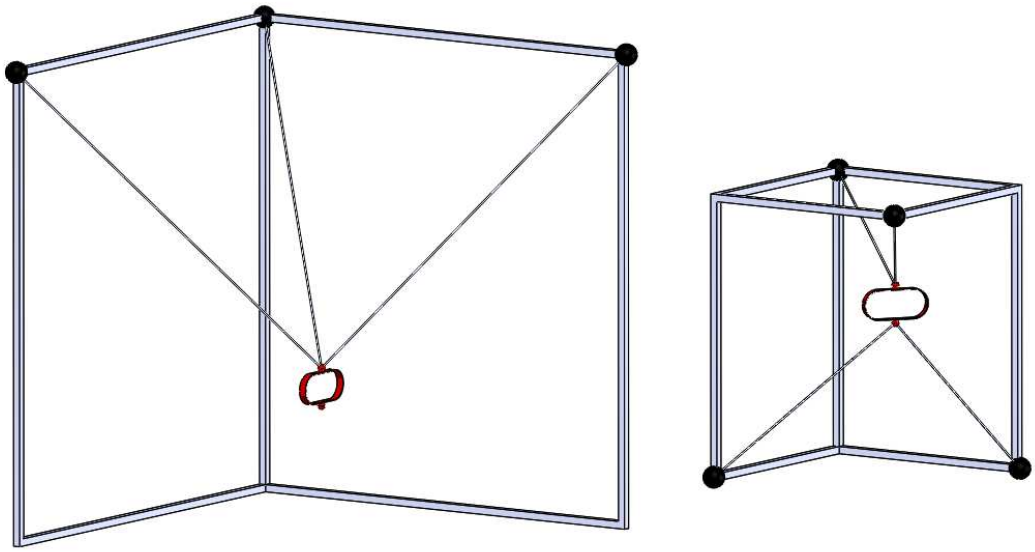

(a) (b)

Fig. 25. (a) CAD of the built LAWEX prototype, (b) CAD of the proposed solution

Table 8. Performances comparison of LAWEX prototype and the proposed solution

	LAWEX prototype	Proposed solution	% improvement
Occupied volume	$V_{LAWEX} = 0.234\ \text{m}^3$	$V_{sol} = 0.0347\ \text{m}^3$	$\frac{V_{LAWEX} - V_{sol}}{V_{LAWEX}}\% = 85\%$
Maximal cable tension	$\text{Max}(\tau_{\text{LAWEX}}) = 20.1\ \text{N}$	$\text{Max}(\tau_{sol}) = 19.7\ \text{N}$	$\frac{\text{Max}(\tau_{\text{LAWEX}}) - \text{Max}(\tau_{\text{sol}})}{\text{Max}(\tau_{\text{LAWEX}})}\% = 2\%$
Safety: minimal distance between cables and the patient	$d_{\min LAWEX} = 10.4\ \text{cm}$	$d_{\min sol} = 6.3\ \text{cm}$	$\frac{d_{\min LAWEX} - d_{\min sol}}{d_{\min LAWEX}}\% = -38\%$

6. Conclusion

First part of this paper focuses at fundamental characteristics related to topological and dimensional performances of CDPRs with a general discussion on their type and dimensional synthesis, which are currently done in sequential order. Then, authors propose a concurrent optimization approach specific for CDPRs, which is combining their type and dimensional synthesis. A specific case of study is carried out by referring to LAWEX a 3DOFs CDPR rehabilitation device for the human forearm. The reported case of study proposes concurrent multi-objective optimization by taking into account cables tensions and occupied volume alongside with desired workspace and motion performances. Topology search has been considering four different topology designs of LAWEX. The topology and dimensions of the mechanism are optimized, simultaneously. In addition to the design parameters, the decision vector of the GA contains a discrete variable to define the selected topology among the four proposed architectures. A Pareto front has been obtained showing the set of feasible optimal solutions. An additional safety criterion is implemented for identifying an optimal solution among the set of solutions in the obtained Pareto front. This has allowed to identify the desired optimal solution. Results demonstrate a 2-2 topology as being the most effective in terms of the selected optimality criteria with optimal tradeoff between occupied robot volume, cable tensions and the user safety.

Acknowledgment

This work is supported by the “Poitiers Université Foundation”.

References

[1] James Albus, R. Bostelman, and N. Dagalakis, "The NIST RoBoCrane," *Journal of research of the National Institute of Standards and Technology*, vol. 94, no. 3, pp. 373–384, 1992.

[2] X. Tang, "An Overview of the Development for Cable-Driven Parallel Manipulator," *Advances in Mechanical Engineering*, vol. January, 2014.

[3] A. M. Pinto, E. Moreira, J. Lima, J. P. Sousa, and P. Costa, "A cable-driven robot for architectural constructions : a visual-guided approach for motion control and path-planning," *Autonomous Robots*, vol. 41, no. 7, pp. 1487–1499, 2017.

[4] G. Billette and C. Gosselin, "Producing Rigid Contacts in Cable-Driven Haptic Interfaces Using Impact Generating Reels," in *IEEE International Conference on Robotics and Automation*, 2009, pp. 307–312.

[5] G. Boschetti, G. Rosati, and A. Rossi, "A haptic system for robotic assisted spine surgery," *Proceedings of the IEEE International Conference on Control Applications*, vol. 24, no. 4, pp. 19–24, 2005.

[6] D. Zanotto, G. Rosati, S. Minto, and A. Rossi, "Sophia-3: A semiadaptive cable-driven rehabilitation device with a tilting working plane," *IEEE Transactions on Robotics*, vol. 30, no. 4, pp. 974–979, 2014.

[7] E. E. Hernández-Martínez, M. Ceccarelli, G. Carbone, C. S. López-Cajún, and J. C. Jáuregui-Correa, "Characterization of a Cable-Based Parallel Mechanism for Measurement Purposes," *Mechanics Based Design of Structures and Machines*, vol. 38, no. 1, pp. 25–49, 2010.

[8] M. J. Varela, M. Ceccarelli, and P. Flores, "A kinematic characterization of human walking by using CaTraSys," *Mechanism and Machine Theory*, vol. 86, pp. 125–139, 2015.

[9] D. Cafolla, M. Russo, and G. Carbone, "CUBE , a Cable-driven Device for Limb Rehabilitation," *Journal of Bionic Engineering*, vol. 16, pp. 493–494, 2019.

[10] C. Fanin, P. Gallina, A. Rossi, U. Zanatta, and S. Masiero, "NeRebot: A Wire-based Robot for Neurorehabilitation.pdf," in *In Proceedings of the 8th International Conference on Rehabilitation Robotics ICORR03*, 2003, pp. 23–26.

[11] G. Rosati, S. Masiero, and A. Rossi, "On the Use of Cable-Driven Robots in Early Inpatient Stroke Rehabilitation," in *Advances in Italian Mechanism Science,Mechanisms and Machine Science 47*, 2017, pp. 551–558.

[12] R. Kelaiaia, O. Company, and A. Zaatri, "Multiobjective optimization of a linear Delta parallel robot," *Mechanism and Machine Theory*, vol. 50, pp. 159–178, 2012.

[13] R. Kelaiaia, A. Zaatri, O. Company, and L. Chikh, "Some investigations into the optimal dimensional synthesis of parallel robots," *International Journal of Advanced Manufacturing Technology*, vol. 83, no. 9–12, pp. 1525–1538, 2016.

[14] M. A. Laribi, L. Romdhane, and S. Zeghloul, "Analysis and dimensional synthesis of the DELTA robot for a prescribed workspace," *Mechanism and Machine Theory*, vol. 42, no. 7, pp. 859–870, 2007.

[15] S. Botello-Aceves, S. I. Valdez, H. M. Becerra, and E. Hernandez, "Evaluating concurrent design approaches for a Delta parallel manipulator," *Robotica*, vol. 36, no. 5, pp. 697–714, 2018.

[16] M. A. Laribi, A. Mlika, L. Romdhane, and S. Zeghloul, "Multi criteria optimum design of 3 dof translational in parallel manipulators (3TPM)," in *13th World Congress in Mechanism and Machine Science*, 2011, pp. 19–25.

[17] T. Essomba, M. A. Laribi, S. Zeghloul, and G. Poisson, "Optimal synthesis of a spherical parallel mechanism for medical application," *Robotica*, vol. 34, no. 3, pp. 671–686, 2016.

[18] N. Bilel, N. Mohamed, A. Zouhaier, and R. Lotfi, "Multi-objective robust design optimization of a mechatronic system with uncertain parameters, using a polynomial chaos expansion method," *Proceedings of the Institution of Mechanical Engineers. Part I: Journal of Systems and Control Engineering*, vol. 231, no. 9, pp. 729–739, 2017.

[19] L. M. Amine, C. Giuseppe, and Z. Saïd, "On the Optimal Design of Cable Driven Parallel Robot with a Prescribed Workspace for Upper Limb Rehabilitation Tasks," *Journal of Bionic Engineering*, vol. 16,

pp. 503–504, 2019.

[20] H. Lamine, M. A. Laribi, S. Bennour, L. Romdhane, and S. Zeghloul, “Design Study of a Cable-based Gait Training Machine,” *Journal of Bionic Engineering*, vol. 14, no. 2, pp. 232–244, 2017.

[21] E. Hernandez, S. I. Valdez, G. Carbone, and M. Ceccarelli, “Design Optimization of a Cable-driven Parallel Robot in Upper Arm Training-Rehabilitation Processes,” in *MuSMe*, 2017, vol. 3, pp. 1–10.

[22] P. Liu and Y. Qiu, “Tension Optimization for a Cable-Driven Parallel Robot with Non- Negligible Cable Mass,” *The Open Automation and Control Systems Journal*, vol. 7, pp. 1973–1980, 2015.

[23] J. E. Parada Puig, N. E. N. Rodriguez, and M. Ceccarelli, “A methodology for the design of robotic hands with multiple fingers,” *International Journal of Advanced Robotic Systems*, vol. 5, no. 2, pp. 177–184, 2008.

[24] D. G. Olson, A. G. Erdman, and D. R. Riley, “A systematic procedure for type synthesis of mechanisms with literature review literaturbe-sprechung,” *Mechanism and Machine Theory*, vol. 20, no. 4, pp. 285–295, 1985.

[25] L. Nouaille, M. A. Laribi, C. A. Nelson, T. Essomba, G. Poisson, and S. Zeghloul, “Design process for robotic medical tool guidance manipulators,” *Proceedings of the Institution of Mechanical Engineers, Part C: Journal of Mechanical Engineering Science*, vol. 230, no. 2, pp. 259–275, 2016.

[26] J-P. Merlet, “On the Redundancy of Cable-Driven Parallel Robots,” in *New Trends in Mechanism and Machine Science. Mechanisms and Machine Scienc*, vol. 24, no. september, P. Flores and F. Viadero, Eds. Springer, Cham, 2014, pp. 31–39.

[27] M. A. Khosravi and H. D. Taghirad, “Robust PID control of fully-constrained cable driven parallel robots,” *Mechatronics*, vol. 24, no. 2, pp. 87–97, 2014.

[28] M. Gouttefarde and C. M. Gosselin, “Analysis of the wrench-closure workspace of planar parallel cable-driven mechanisms,” *IEEE Transactions on Robotics*, vol. 22, no. 3, pp. 434–445, 2006.

[29] J. M. Heo, B. J. Park, J. O. Park, C. S. Kim, J. Jung, and K. S. Park, “Workspace and stability analysis of a 6-DOF cable-driven parallel robot using frequency-based variable constraints,” *Journal of Mechanical Science and Technology*, vol. 32, no. 3, pp. 1345–1356, 2018.

[30] A. Z. Loloei, M. M. Aref, and H. D. Taghirad, “Wrench feasible workspace analysis of cable-driven parallel manipulators using LMI approach,” in *IEEE/ASME International Conference on Advanced Intelligent Mechatronics, AIM*, 2009, pp. 1034–1039.

[31] G. Castelli, E. Ottaviano, and M. Ceccarelli, “A fairly general algorithm to evaluate workspace characteristics of serial and parallel manipulators,” *Mechanics Based Design of Structures and Machines*, vol. 36, no. 1, pp. 14–33, 2008.

[32] I. Ben Hamida, M. A. Laribi, A. Mlika, L. Romdhane, and S. Zeghloul, “Geometric Based Approach for Workspace Analysis of Translational Parallel Robots,” in *ROMANSY 22 – Robot Design, Dynamics and Control. CISM International Centre for Mechanical Sciences*, 2019, vol. 584, pp. 180–188.

[33] M. A. Laribi, A. Mlika, L. Romdhane, and S. Zeghloul, “Geometric and Kinematic Performance Analysis and Comparison of Three Translational Parallel Manipulators,” in *The 14th IFToMM World Congress*, 2015.

[34] J. W. Jeong, S. H. Kim, Y. K. Kwak, and C. C. Smith, “Development of a parallel wire mechanism for measuring position and orientation of a robot end-effector,” *Mechatronics*, vol. 8, no. 8, pp. 845–861, 1998.

[35] K. Kozak, Q. Zhou, and J. Wang, “Static analysis of cable-driven manipulators with non-negligible cable mass,” *IEEE Transactions on Robotics*, vol. 22, no. 3, pp. 425–433, 2006.

[36] C. A. Nelson, M. A. Laribi, and S. Zeghloul, “Optimization of a Redundant Serial Spherical Mechanism for Robotic Minimally Invasive Surgery,” in *Computational Kinematics. Mechanisms and Machine Science*, vol. 50, L. M. Zeghloul S., Romdhane L., Ed. Springer,Cham, 2018, pp. 126–143.

[37] I. Ben Hamida, M. . Laribi, A. Mlika, L. Romdhane, and S. Zeghloul, “Comparative Study of Design of a 3-DOF Translational Parallel Manipulator with Prescribed Workspace,” in *Advances in Mechanism*

and Machine Science. IFToMM WC 2019, Mechanisms and Machine Science, vol. 73, T. UHL, Ed. Springer, Cham, 2019, pp. 501–512.

[38] X. Diao, O. Ma, and Q. Lu, "Singularity analysis of planar cable-driven parallel robots," in *IEEE International Conference on Robotics, Automation and Mechatronics*, 2008, pp. 272–277.

[39] J. P. Merlet, "Singularity of cable-driven parallel robot with sagging cables: Preliminary investigation," in *International Conference on Robotics and Automation*, 2019, vol. 2019–May, pp. 504–509.

[40] C. Gosselin and J. Angeles, "A Global Performance Index for the Kinematic Optimization of Robotic Manipulators," *Journal of Mechanical Design*, vol. 113, no. September 1991, p. 220, 1991.

[41] ISO/TC 299 ROBOTICS, "Particular requirements for basic safety and essential performence of medical robots for rehabilitation, assessment, compensation or alleviation," in *medical electrical equipment*, 1st ed., 2019.

[42] C. Giuseppe, B. Gherman, I. Ulinici, and C. Vaida, "Design Issues for an Inherently Safe Robotic Rehabilitation Device," in *Advances in Service and Industrial Robotics. RAAD 2017. Mechanisms and Machine Science. vol 49*, C. Ferraresi and G. Quaglia, Eds. Springer, Cham, 2017, pp. 1025–1032.

[43] G. Boschetti, G. Carbone, and C. Passarini, "Cable Failure Operation Strategy for a Rehabilitation Cable-Driven Robot," *Robotics*, vol. 8, no. 1, pp. 1–12, 2019.

[44] I. Ben Hamida, M. A. Laribi, A. Mlika, L. Romdhane, S. Zeghloul, and G. Carbone, "Novel Safety Criterion for Synthesis of Cable Driven Parallel Robots," in *Mechanisms and Machine Science*, vol. 84, 2020, pp. 112–120.

[45] M. H. Rahman, M. Saad, J. P. Kenné, and P. S. Archambault, "Exoskeleton robot for rehabilitation of elbow and forearm movements," in *18th Mediterranean Conference on Control and Automation, MED'10*, 2010, pp. 1567–1572.

[46] M. H. Rahman, M. Saad, J. P. Kenné, and P. S. Archambault, "Modeling and control of a 7DOF exoskeleton robot for arm movements," in *IEEE International Conference on Robotics and Biomimetics, ROBIO*, 2009, pp. 245–250.

[47] S. Plagenhoef, F. G. Evans, and T. Abdelnour, "Anatomical Data for Analyzing Human Motion," *Research Quarterly for Exercise and Sport*, vol. 54, no. 2, pp. 169–178, 1983.

[48] K. Deb, S. Agrawal, A. Pratap, and T. Meyarivan, "A fast elitist non-dominated sorting genetic algorithm for multi-objective optimization: NSGA-II," *Lecture Notes in Computer Science (including subseries Lecture Notes in Artificial Intelligence and Lecture Notes in Bioinformatics)*, vol. 1917, pp. 849–858, 2000.